

# GROWTH AND CHARACTERIZATION OF A NEW ORGANIC- ORGANIC NLO MATERIAL

G. Indramahalakshmi

Faculty of Chemistry, Cardamom Planters Association College,  
Bodinayakanur – 625 513, Tamil Nadu, India.

## ABSTRACT

A new NLO material of *para*-toluenesulfonic acid with semicarbazide is synthesized and optical quality single crystal was grown by slow evaporation technique. The FT-IR study substantiated the formation of anion and cation by proton shift from PTSA to semicarbazide resulting in adduct formation. Vibrations due to all functional groups appeared in their respective regions confirming adduct formation. All the signals in  $^{13}\text{C}$  NMR spectrum correlate very well with the proposed structure with 1:1 molecular formula ratio. UV-Vis-DRS transmission studies show that the grown crystal has optical transparency around 80%. The cut-off wavelength and band gap energy were found to be 265 nm and 4.31 eV respectively. The emission spectrum indicates that the sample exhibits blue lighting emission sharply at 445 nm and it will be useful for fabricating blue light emitting diodes.

**Keywords:** Semicarbazide *para*-toluenesulfonate, Tauc Graph, Meyer's Index,  $^1\text{H}/^{13}\text{C}$  NMR.

## INTRODUCTION

The family of organic-organic hybrid salts have attracted much attention due to their novel and interesting properties, potential applications in optical data storage, color displays, optical communications, efficient Raman lasers and second harmonic generators<sup>1-3</sup>, and nonlinear optical materials (NLO). The main steering force of such molecular solids is the hydrogen bonding that decides the application of these materials.

*Para*-toluenesulfonic acid (PTSA) is a strong organic acid, a million times stronger than benzoic acid non-oxidizing and is used in organic synthesis, as an "organic-soluble" acid catalyst. Its metal salts, are often used as components of dyed paper and color stabilizers for ink-jet printing sheets. It has commercial importance as a potent and durable calcium channel blocker. Semicarbazide [ $\text{NH}_2\text{NHCONH}_2$ ] is a derivative of urea. Semicarbazide products are known to have activities of antiviral, anti-infective and anti-neoplastic through binding to copper or iron metal atoms in cells. It is used in preparing pharmaceuticals including nitrofurans antibacterials and related compounds. Semicarbazide is also used as a detection reagent on thin layer chromatography (TLC).

Semicarbazide stains  $\alpha$ -keto acids on the TLC plate, which must then be viewed under a UV light to see the results. Most of the semicarbazide adducts are those formed with aldehydes and proteins<sup>4,5</sup>. PTSA has been reported to form an adduct with betaine<sup>6</sup> and glycine<sup>7</sup>. So, the aim of the present work is to synthesize and characterize a new NLO material from PTSA and semicarbazide.

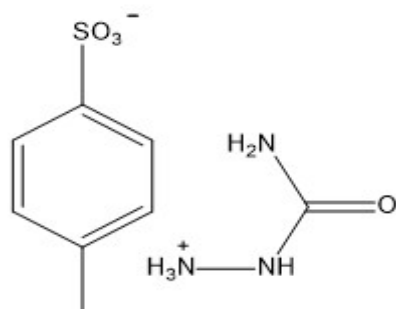
## EXPERIMENTAL

The synthesis of the adduct semicarbazide *para*-toluenesulfonate (**SPTS**) was carried out by the mixing equal volumes of aqueous solutions of 0.5 M PTSA and semicarbazide in 50 ml of water. After concentration to 40 ml, partial room temperature evaporation of the hot filtered solution yielded large colorless crystals within three days. Elemental analysis was carried out in elemental vario EL III germany. The  $^1\text{H}$  NMR and  $^{13}\text{C}$  NMR spectras are recorded in Bruker DPX 400 instrument ( $^1\text{H}$  400 MHz,  $^{13}\text{C}$  75.32 MHz) in  $\text{D}_2\text{O}$ . The IR spectra is recorded as KBr pellets using JASCO 640 Plus Spectrometers in 4000-400  $\text{cm}^{-1}$  region with the resolution of 4  $\text{cm}^{-1}$ . The electronic spectra is recorded as KBr pellets using a JASCO 530V UV-Visible

Spectrophotometer in the range of 200-1000 nm.

## RESULTS AND DISCUSSION

The calculated/ observed values of elements present are C= 38.86/ 38.36, H= 5.26/ 5.01, N= 17.00/ 17.34, S= 12.95/ 12.60, O= 25.91/ 25.86%. Thus the compound has 1:1 molecular formula ratio. The compound is soluble in coordinating solvents like water, DMSO, MeOH and has the possible structure.



### 1. Crystal Growth

Solubility studies were carried out using the synthesized salt of SPTS and double distilled water as solvent. Saturated solution was prepared at various temperatures (30- 45°C) with the help of a constant temperature bath ( $\pm 0.01$  °C) and the amount of solute was measured gravimetrically. The variation of solubility with temperature is given in Fig.1 which shows that the solubility increases linearly with temperature, exhibiting a high solubility coefficient. Bulk single crystals of SPTS were grown by slow evaporation technique from aqueous solution. Single crystals of SPTS obtained are shown in Fig. 2.

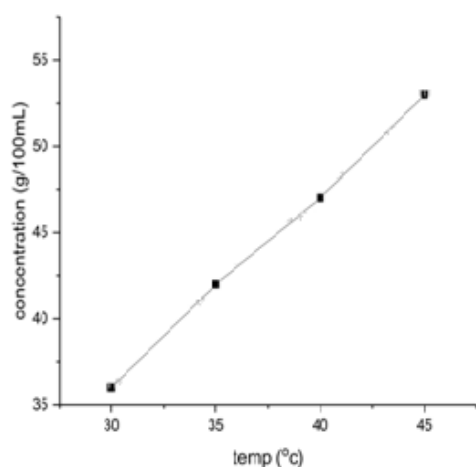


Fig.1: Solubility curve of SPTS



Fig. 2: Photograph of SPTS crystal

### 2. Absorption spectral analysis

The absorption spectrum of SPTS (Fig.3) shows intense bands centered at 240 and 264 nm, attributed to  $n-\pi^*/\pi-\pi^*$  transition of the  $\text{C=O}$  and  $\pi-\pi^*$  transition of the benzene ring respectively. The crystal has lower cut-off wavelength at 240 nm which is less than that of glyciniun nitrate crystals<sup>8</sup>. There was no absorption band beyond 264 nm, which confirmed the absence of any overtones. Also low absorbance behavior shows the colorless nature of the crystal.

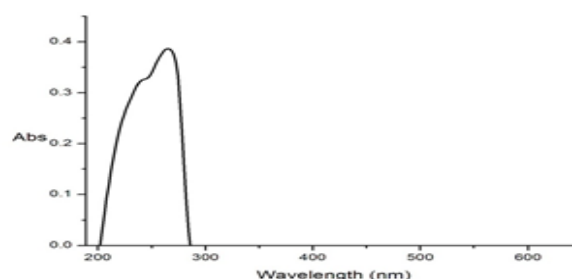


Fig. 3: UV Spectrum of SPTS

### 3. UV DRS

The optical transmittance of SPTS powder was measured using JASCO UV VIS & DRS V-750 spectrophotometer in the range of 190-900 nm and is shown in Fig.4. Similar transmittance window in the visible region enables good optical transmission of the second harmonic frequencies of Nd: YAG laser<sup>9</sup>. Hence, the present adduct qualifies itself for possible use as NLO applications. So SPTS crystal could be used for generation and mixing of frequencies over a wide range of electromagnetic spectrum including the UV and for blue green laser application<sup>10</sup>. The optical band gap ( $E_g$ ) was evaluated from the transmission spectrum and the optical

absorption coefficient ( $\alpha$ ) near the absorption edge was estimated by using the relation,  $(\alpha h\nu) = A (E_g - h\nu)^{1/2}$  where  $A$  is a constant,  $E_g$  is the optical band gap. The Tauc's graph plotted between the product of absorption coefficient and the incident photon energy  $(\alpha h\nu)^2$  with the photon energy  $(h\nu)$  shows a linear behavior that can be considered as evidence for the direct transition (Fig.5). The band gap value has been obtained by extrapolating the linear portion of the plot to intercept the photon energy axis and found to be 4.31eV. The wide optical energy band gap of the grown crystal confirms that the SPTS crystal possess large transmittance in the visible region.

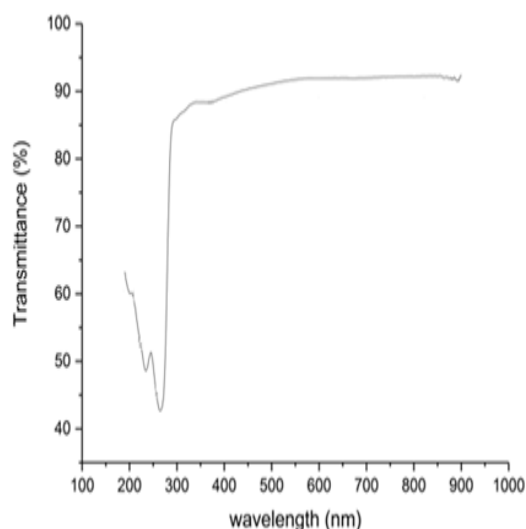


Fig. 4: UV DRS Spectrum of SPTS

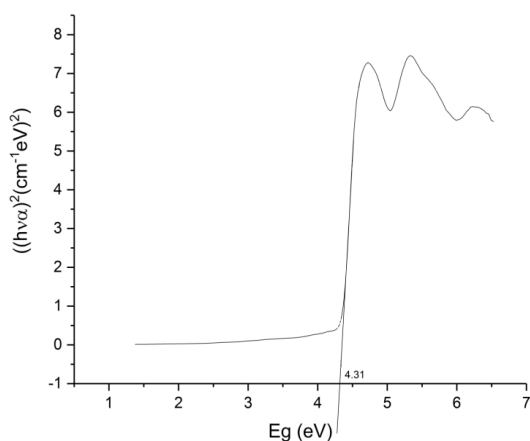


Fig. 5: Tauc Graph of SPTS

#### 4. IR spectrum analysis

The infrared spectrum of the compound is presented in Fig. 6 and the vibrational frequencies are given in Table 1. A band in the range  $2923 \text{ cm}^{-1}$  can be assigned to the stretching vibration of the  $(\text{CH}_3)$  group. The band around  $1384 \text{ cm}^{-1}$  is due to the symmetric deformation of methyl group. The peaks due to  $\nu(\text{C}=\text{C})_{\text{ar}}$ ,  $1627$  and  $1497 \text{ cm}^{-1}$  show the presence of benzenoid ring. A strong band observed at  $1135 \text{ cm}^{-1}$  ( $\beta\text{CH}_{\text{ar}}$ ) coincides well with the literature values observed in the range  $1220\text{-}1120 \text{ cm}^{-1}$  and is considered to be a measure of the degree of delocalization of electrons due to hydrogen bonding with the oxygen atoms in the  $\text{SO}_3^-$  group and thus it is a characteristic peak of PTSA in the adduct. The three bands appearing at  $822$ ,  $860$  and  $956 \text{ cm}^{-1}$  are attributed to out of plane (C-H) bending vibrations ascribed to the *para* substituted aromatic rings<sup>12</sup>. A very strong band at  $799 \text{ cm}^{-1}$  is assigned to the ring breathing mode in agreement with that ( $800 \text{ cm}^{-1}$ ) for a number of *para*-substituted benzene derivatives<sup>11,13</sup>. It is well documented that sulfonic acids have a strong, broad and split bands in the region of  $1000 - 1250 \text{ cm}^{-1}$ <sup>11,14</sup>. The mode at  $1033 \text{ cm}^{-1}$  can be assigned to  $\text{SO}_3^-$  group of the PTSA as reported in<sup>15</sup>, confirming presence of PTSA in the adduct. The stretching vibrations of amino group ( $\text{NH}_2$ ) usually appear in the range of  $3500\text{-}3300 \text{ cm}^{-1}$ . The  $\text{NH}_2$  group in the compound exhibits the above peak at  $3441$  and  $3203 \text{ cm}^{-1}$ . The symmetric stretching mode of  $^+\text{NH}_3$  is normally observed in the region  $2600\text{-}2800 \text{ cm}^{-1}$ <sup>16</sup>. The appearance of two strong peaks at  $2724$ ,  $2765 \text{ cm}^{-1}$  shows the existence of  $^+\text{NH}_3$ . This proves the protonation of  $\text{NH}_2$  group in the compound. The observed bunch of peaks in the region  $2700\text{-}3500 \text{ cm}^{-1}$  due to the presence of various groups like  $\text{NH}$ ,  $\text{NH}_2$ ,  $^+\text{NH}_3$ ,  $\text{CH}$  and  $\text{CH}_3$  in the adduct, is favoring the structure,  $^+\text{NH}_3\text{-NH-CO-NH}_2\text{---PTSA}$ . The bending vibrations of amino group in various forms occur at  $1714$ ,  $1627$  and  $1539 \text{ cm}^{-1}$ . As the characteristic infrared absorption frequencies of  $\text{C}=\text{O}$  in amides are normally strong in intensity and recorded in the region  $1690\text{-}1630 \text{ cm}^{-1}$ <sup>17</sup>, the band at  $1660 \text{ cm}^{-1}$  is assignable to the  $\text{C}=\text{O}$  group.

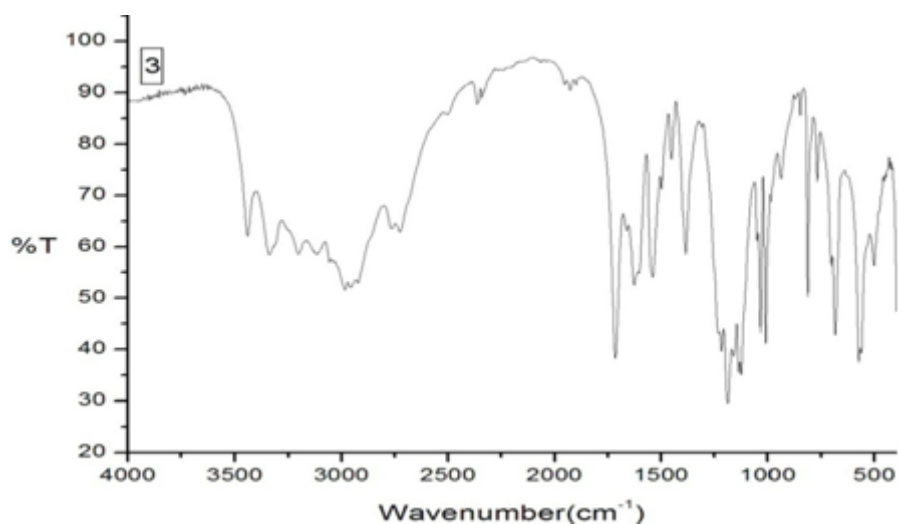


Fig. 6: FT-IR Spectrum

Table 1: FT-IR Spectral assignments for SPTS

SPTS	Assignments	SPTS	Assignments
3441 s	$\nu_a$ NH	1451 m	$\delta_s$ C-CH <sub>3</sub>
3203 s	$\nu_s$ N-H	1384 m	$\delta$ CH <sub>3</sub>
3057 s	$\nu$ CH $\phi$	1307 w	$\nu$ CN
3038 s	$\nu$ CH $\phi$	1158 s	$\nu_{as}$ SO <sub>3</sub> , $\beta$ CH $\phi$ ,
2923 s	$\nu_a$ CH <sub>3</sub>	1135 s	$\beta$ CH $\phi$
2765 m	$\nu$ NH <sub>3</sub> <sup>+</sup>	1033 s	$\delta$ CH <sub>3</sub> , $\nu_s$ SO <sub>3</sub> , $\nu$ CN
2724 s			
1714 s	$\nu$ C=O, $\delta$ NH <sub>2</sub>	1009 s	$\nu$ C-N
1660 m	$\nu$ C=O, $\delta$ NH <sub>2</sub>	814 s	$\gamma$ CH $\phi$
1627 s	$\nu$ (C=C) $\phi$ , $\delta$ NH <sub>2</sub>	685 s	$\nu$ C-S, $\gamma$ NH <sub>2</sub>
1539 s	$\nu$ (C=C) $\phi$ , $\delta$ NH <sub>2</sub> , $\nu$ C=O	563 s	$\nu\phi_{skel}$ , $\delta\phi$ CCC, $\rho$ , SO <sub>3</sub> , $\delta$ CN
1497 m	$\nu$ (C=C) $\phi$ , $\delta_{as}$ CH <sub>3</sub> , $\nu$ (N-C-N)	490 s	$\delta$ NH <sub>3</sub> , $\delta$ CN, $\delta$ (N-C-N)

### 5. NMR Spectral analysis

The <sup>1</sup>H and <sup>13</sup>C NMR spectrum data are presented in Table 2. All the signals correlate very well with the proposed structure.

Table 2: <sup>1</sup>H and <sup>13</sup>C NMR spectroscopic data in (D<sub>2</sub>O)

<sup>1</sup> H NMR		<sup>13</sup> C NMR	
7.5	2H, Aro	142	1C, C-S
7.11	2H, Aro	139	1C, C-CH <sub>3</sub>
2.13	3H, CH <sub>3</sub>	129	2C, Aro
7.48	3H, NH <sub>3</sub> <sup>+</sup>	125	2C, Aro
4.70	NH <sub>2</sub> , NH merges with the solvent	20.4	1C, CH <sub>3</sub>
		159	C=O

### 6. Micro hardness Measurements

Micro hardness testing is one of the best methods for understanding the mechanical properties of materials<sup>18</sup>. Hardness of the material is a measure of resistance, that offers to deformation<sup>19</sup>. The transparent polished crystal free from cracks was selected for hardness measurements. The indentations were made on the flat surface with the load ranging from 25 to 100 g using Shimadzu make-model-HMV-2 fitted with Vicker's pyramidal indenter and attached to an incident light microscope. The indentation time was kept as 5seconds for all the loads. The

Vickers's hardness number  $H_v$  was calculated from the following expression.  $H_v = (1.8544 P)/d^2$  kg/mm<sup>2</sup> where P is the applied load in kg and d is the diagonal length of the indentation impression in millimeter and 1.8544 is a constant of a geometrical factor for the diamond pyramid. A plot obtained between the hardness number and the load is shown in Fig.7. The relation connecting the applied load and diagonal length 'd' of the indenter is given by Meyer's law  $P = ad^n$ , where n is the Meyer's index or work hardening coefficient. A plot obtained between log (P) and log (d) gives a straight line. Meyer's index is calculated from

the slope of straight line. From many observations on various materials Onitsch<sup>20</sup> pointed out that 'n' lies between 1 and 1.6 for moderately hard materials, and it is more than 1.6 for soft materials, The observed value of Meyer's index for SPTS is 3 and hence SPTS belongs to the soft materials category.

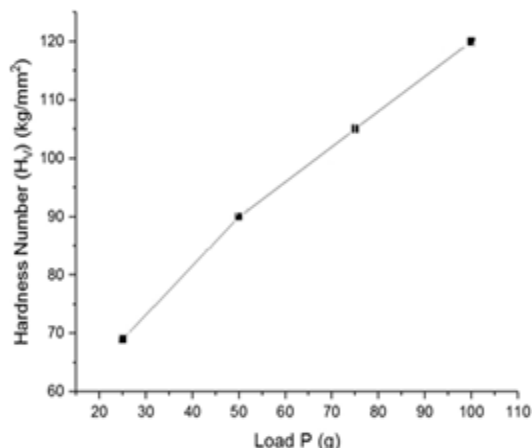


**Fig. 7: Plot of Vicker's hardness for SPTS**

### 7. Powder SHG Measurements

SHG may be used as a tool to evaluate at least qualitatively the bulk homogeneity of the samples under investigation<sup>21</sup>. A quantitative measurement of the second harmonic generation (SHG) efficiency of SPTS crystal was determined by the modified version of powder technique developed by Kurtz and Perry<sup>22</sup>. The SPTS crystal was made into powder and it was packed densely between two transparent glass slides. A high intensity Nd: YAG laser (1064nm) was passed through the pelletized sample. The SHG behavior is confirmed from the output of the laser beam having the bright blue emission ( $\lambda = 445$  nm) from the crystal. KDP crystal was powdered to the identical size of SPTS and was used as reference material in the SHG measurement. The SHG efficiency of SPTS (10 mV) is approximately 0.5 times that of KDP (22 mV).

### CONCLUSION

Nonlinear optical organic single crystal was grown by slow evaporation technique. 1:1 molecular formula ratio was obtained from elemental analysis. Infrared spectral study was used to confirm the functional groups present in the compound. The cut-off wavelength and band gap energy were found to be 265 nm and 4.31 eV respectively. The wide optical energy band gap of the grown crystal confirms that the SPTS crystal possess large transmittance in the visible region. The FT-IR and NMR studies substantiated the formation of anion and cation by proton shift from PTSA to semicarbazide resulting in adduct formation.

The absorption spectrum shows 80% optical transmittance in the entire region. Thus the new material qualifies itself for possible use as NLO applications.

### REFERENCES

1. Dmitriev VG, Gurzadyan GG and Nicogosyan DN. Handbook of Nonlinear Optical Crystals, Springer-Verlag, Newyork, 1999.
2. Razze C, Ardyno M, Zanotti L, Zha M, Paorici C. Cryst Res Technol. 2002;37:456.
3. Wong MS, Bosshard C, Pan F and Gunter P. Adv Mater. 1996;8:677.
4. De biase D, Agostinelli E, De matteis G, Mondov B and Morpurgo L. Eur J Biochem. 1996;237: 93-99.
5. Read WA and Castle L. Central Science Laboratory, York; &L. Coulier, E.K. Zondervan-van Beuken, M.A.H. Rijk, TNO Nutrition and Food Research, The Netherlands; 2003, Project a03037.
6. Haussuhl S and Kristallogr Z. 1989;188:311.
7. Chwaleba D, Ilczyszyn M and Ciunik Z. J Molecular Struct. 2007;831:119.
8. Martin BrittoDhas SA and Natarajan S. Growth and characterization of a new organic NLO material: Glycine nitrate, Optics communications. 2007;278:434.
9. Rao CNR. Ultraviolet and visible spectroscopy of organic compound, Prentice Hall of India Pvt. Ltd. New Delhi, 1984.
10. Krishna Rao K, Surender V and Savitharani B. Bull Mater Sci. 2002;25:641-646.
11. Ljupco Pejov, Mirjana Ristova and Bojan Soptrajanov. Spectrochimica Acta PartA. 2011;79: 27.
12. Amalraj John, Palamari JayaPrakash Yadav and Srinivasan Palaniappan. J Molecular Catalysis A: Chemical. 2006;248:121.
13. Singh DN and Yadav RA. Asian Chem Lett. 1998;2:65.
14. Socrates G. Infrared and Raman characteristic Group Frequencies, Edn - 3, John Wiley & Sons: Chichester. 2001 and references therein.
15. Lorenc J, Bryndal I, Marchewka M, Sasidek W, Lis T and Hanuza J. J Raman Spectrosc. 2008;39:569.
16. Gunasekaran S, Anand G, Arun Balaji R, Dhanalakshmi J, Kumaresan S and Anbalagan G. Int J ChemTech Res. 2009;1(3):649.
17. Silverstein RM and Webster FX. Spectrometric Identification of Organic

- Compounds, sixth ed., John Wiley & Sons, Inc. 1998.
18. Lal B, Bamzai KK and Kotru PN. Mater Chem Phys. 2003;78:202-207.
  19. Mott BW. Micro Indentation Hardness Testing, Butterworths, London, 1956.
  20. Onitsch EM. Mikroskopie. 1950;95:12-14.
  21. Sherwood JN. Philos Trans R Soc London. 1990;A330:127.
  22. Kurtz SK and Perry TT. J Apply Phys. 1968;39:3798-3813.